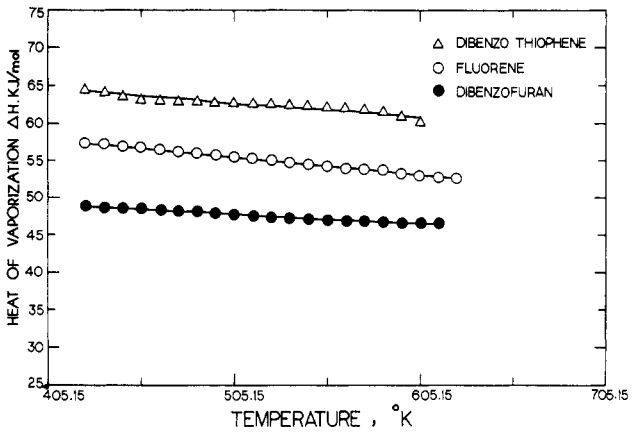

Figure 5. Heats of vaporization of fluorene, dibenzofuran, and dibenzothiophene.

In the case of dibenzofuran, the heat of vaporization has been observed to be smaller than that of fluorene.

Acknowledgment

We thank Mr. Ray Martin for his valuable assistance during modification of the equipment.

Literature Cited

(1) American Petroleum Institute. "Selected Values of Properties of Hydrocarbons and Related Compounds"; Chem. Thermodynamic Prop. Center, API Research Project 44, Texas A & M University: College Station, TX, 1971.
(2) Rieveschl, G.; Ray, F. E. *Chem. Rev.* **1938**, *23*, 287.
(3) Edwards, D. R.; Prausnitz, J. M. *J. Chem. Eng. Data* **1981**, *26*, 121.
(4) Taylor, W. J.; Rossini, F. D. *J. Res. Natl. Bur. Stand. (U.S.)* **1944**, *32*, 197.
(5) Nasir, P.; Hwang, S. C.; Kobayashi, R. *J. Chem. Eng. Data* **1980**, *25*, 298.
(6) Ruska, W. E. A.; Hurt, L. J.; Kobayashi, R. *Rev. Sci. Instrum.* **1970**, *41*, 1444.
(7) Wieczorek, S. A.; Kobayashi, R. *J. Chem. Eng. Data* **1980**, *25*, 302.
(8) Ambrose, D.; Counsell, J. F.; Davenport, A. J. *J. Chem. Thermodyn.* **1970**, *2*, 283.
(9) Wilson, G. M., et al. *Ind. Eng. Chem. Process Des. Dev.* **1981**, *20*, 94.
(10) Mortimer, S. F.; Murphy, R. V. *J. Ind. Eng. Chem.* **1923**, *15*, 1140.
(11) Pitzer, K. S.; Lippmann, D. Z.; Curl, R. F., Jr.; Huggins, C. M.; Peterson, E. D. *J. Am. Chem. Soc.* **1955**, *77*, 3433.
(12) Wieczorek, S. A.; Kobayashi, R. *J. Chem. Eng. Data* **1981**, *26*, 11.
(13) "Coal Tar Data Book", 2nd ed.; Coal Tar Research Association: Gomersal, Leeds, England, 1965.

Received for review October 6, 1981. Accepted March 26, 1982. We acknowledge EPRI and the Phillips Petroleum Co. for their financial support of this project.

Thermophysical Properties of the Equimolar Mixture $NaNO_3$–KNO_3 from 300 to 600 °C

Donald A. Nissen

Exploratory Chemistry Division I, Sandia National Laboratories, Livermore, California 94550

The thermophysical properties (viscosity, surface tension, and density) of the equimolar mixture $NaNo_3$–KNO_3 have been determined over the temperature range 300–600 °C in argon and in oxygen. The surface tension is a linear function of the temperature and can be represented by the expression γ(dyn/cm) = 133.12 – (6.25 × 10^{-2})T(°C). The viscosity may be calculated from the equation η(cP) = 22.714 – 0.120T + (2.281 × 10^{-4})T^2 – (1.474 × 10^{-7})T^3, for T in °C. The density of the equimolar mixture is given by ρ(g/cm^3) = 2.090 – (6.36 × 10^{-4})T(°C). In contrast to the surface tension and the viscosity, the density is affected by the presence of nitrite, the thermal decomposition product of the nitrate anion.

The equimolar molten salt mixture $NaNO_3$–KNO_3 is being proposed as a heat-transfer fluid and a thermal-energy storage medium for various solar energy applications. In these applications the maximum operating temperature will be in the range 500–600 °C. Industrial experience and previous experimental investigations on this molten salt mixture have generally been confined to temperatures below 450 °C. In order to provide data to solve various specific design problems associated with the use of these molten nitrate salts as heat-transfer fluids, it is important that we know how the physical properties of these salts are affected by temperature and composition of the liquid and gas phases. It is the purpose of this report to present and comment on the viscosity, surface tension, and density data which we have measured for equimolar $NaNO_3$–KNO_3 over the temperature range 300–600 °C. The implications of these data, insofar as they reflect interactions which may be taking place in the melt, will be discussed elsewhere.

Apparatus and Experimental Technique

The thermophysical-property data for the equimolar $NaNO_3$–KNO_3 mixture were taken by an instrument designed and built by the author at SNLL. This instrument is based on the principle of a damped, one-dimensional, harmonic oscillator, i.e., the motion of a body suspended from a spring and oscillating in a fluid. A description of the theoretical principles which govern the operating of this instrument, the details of construction, and its operation and response are discussed elsewhere (*1*, *2*). Only an abbreviated description of the various modes of operating of this instrument will be given here.

The heart of the apparatus is a quartz spring oscillator, an electromagnet for remotely starting the spring oscillating, a position transducer for remote readout of the spring extension (linear variable differential transformer (LVDT)), and a gold plate suspended in a liquid whose viscosity is being measured (see Figure 1). It is the viscous drag exerted on this plate by the liquid which causes damping of the oscillatory motion of the quartz spring.

The rate of damping of the oscillations of the spring is given by the quantity δ, the logarithmic decrement, where

$$\delta = \frac{1}{n} \ln \frac{y_0}{y_n} \quad (1)$$

where y_0 and y_n are the amplitudes of the zeroth and nth

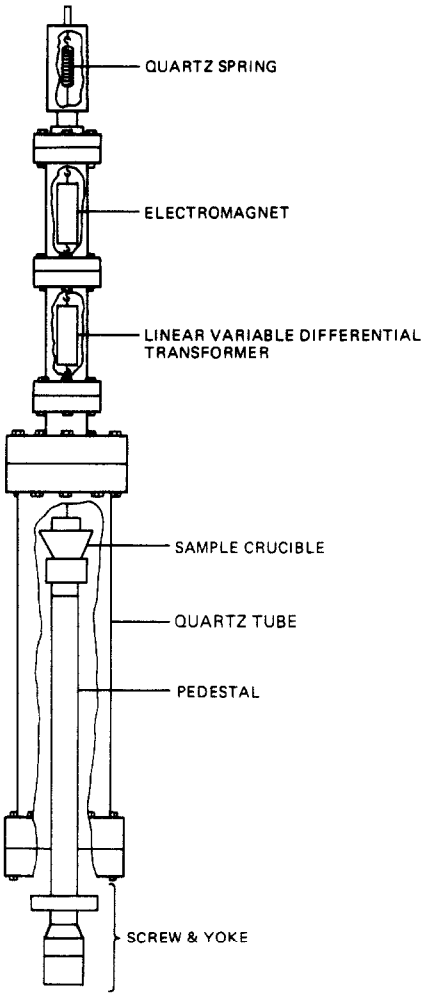

Figure 1. Experimental apparatus (cutaway).

successive oscillation. The viscosity of the liquid may then be calculated from the equation

$$(\eta\rho)^{1/2} = C\delta - E \tag{2}$$

where η and ρ are the viscosity and the density of the liquid being studied and D and E are instrument constants (*2*).

In addition to functioning as a viscometer, the apparatus can be converted to an instrument for measuring surface tension (*1*).

By slowly and continuously separating the liquid and the plate immersed in it, and measuring the maximum force exerted on the plate (which occurs just before the column of liquid supported by the plate breaks), one can determine the surface tension of the liquid by the formula

$$\gamma = \frac{F}{(P \cos \theta)} \tag{3}$$

where γ is the surface tension, F is the maximum force exerted on the plate, which is detected as an apparent increase in the weight of the plate, P is the perimeter of the plate, and θ is the wetting angle, generally assumed to be zero if the liquid wets the plate. The gold plate in these experiments was 1.609 cm wide and 0.0262 cm thick.

The apparatus can also function as an Archimedean densitometer (*1*). The loss in weight (Δw) of a solid of known volume (V) is related to the density of the liquid (ρ) in which it is immersed by

$$\rho = \Delta w / V \tag{4}$$

Therefore, the density of a liquid is given simply by the difference in LVDT reading, converted to weight, with and without liquid surrounding the solid, divided by its volume. For increased accuracy of the density measurements, the thin plate was replaced by a larger volume bob. The bob presently used is made of gold-plated zirconium and is in the form of a right circular cylinder with a tapered top and bottom to permit drainage. A small post with a hole drilled through it extends from the top taper to provide a means of attaching the bob to the LVDT.

For measurements of density using Archimedes' method, it is necessary that the volume of the immersed body be accurately known. This was determined by immersing the bob in several liquids of known density. The volume of the bob was determined to be 1.3518 ± 0.005 cm^3 (*1*).

The liquid being studied is contained in a gold crucible mounted on a pedestal fastened to a screw and yoke arrangement. This is attached to the bottom flange of an intermediate quartz tube. The pedestal and the screw are connected by a machined stainless-steel rod which passes through a compression fitting designed to maintain the integrity of the atmosphere within the viscometer. This arrangement permits the crucible and its contents to be raised or lowered smoothly and slowly about 4 cm. It is the ability to lower the crucible which is central to the surface tension measurement.

A thermocouple sheathed in stainless steel is fed through a fitting in the bottom flange and bent to allow its tip to be immersed in the liquid. In this way the temperature of the liquid can be monitored continuously. A gold sheath on the tip of the thermocouple prevents any reaction between it and the liquid. The bottom flange also has a tube welded into it for admitting gas into the heated zone.

A clam-shell-type furnace, mounted on the supporting structure, is fastened around the quartz tube to heat the contents of the crucible. This furnace and its associated I8478 based coprocessor controller is capable of maintaining the temperature of the crucible content to within ±0.5 °C. The vertical temperature gradient over the 5-cm height of the crucible is <0.5 °C.

The $NaNO_3$ and KNO_3 in these experiments were recrystallized from distilled water at least once and vacuum dried at 150 °C before use. At the conclusion of each experiment, the salt was analyzed for its nitrite content. This analysis involved the oxidation of the NO_2^- by Ce(IV) and back-titrating with oxalate. A more complete discussion of this method is given in ref *3*. Where they are available, literature values are compared with our data.

Results and Discussion

The thermophysical properties that we determined for the equimolar $NaNO_3$–KNO_3 mixture are presented and discussed in this section. These data cover the range 300–600 °C and were taken in argon and in oxygen.

It has been shown (*4*) that heating nitrates to temperatures in the range 500–600 °C results in the formation of significant (~10 wt %) quantities of nitrite. As a consequence of the thermal decomposition of nitrate

$$NO_3^- \leftrightarrow NO_2^- + {}^1/_2O_2 \tag{5}$$

the quantity of nitrate formed is a function of the temperature and oxygen partial pressure (*4*). Because the presence of nitrite may have an effect on the thermophysical properties of the $NaNO_3$–KNO_3 melt, the surface tension, the viscosity, and the density of $NaNO_3$–KNO_3 melts containing 10, 20, and 40 mol % KNO_2 were investigated. It was found that, with the exception of the density, the thermophysical properties were, within the experimental uncertainty, unaffected by the presence of nitrite.

Surface Tension. The experimentally measured surface tension of the equimolar $NaNO_3$–KNO_3 mixture as well as the

Table I. Surface Tension[a] of Equimolar $NaNO_3$-KNO_3

T, °C	γ(exptl), mN/m	γ(ref 6, 7), mN/m	γ(ref 5), mN/m
257	117.1	120.0	117.9
267	116.5	119.2	117.0
280	115.6	118.2	115.7
307	114.4	116.3	114.6
350	111.3	113.0	111.4
400	108.1	109.7	107.7
450	105.0		
500	101.7		
547	109.0		
594	96.0		

[a] 1 mN/m = 1 dyn/cm.

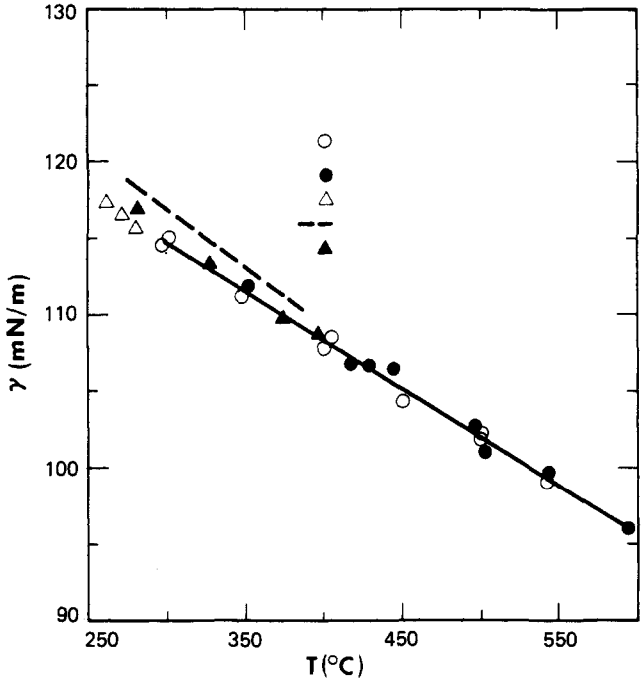

Figure 2. Surface tension of $NaNO_3$–KNO_3 vs. temperature: (O) O_2, (●) Ar, (△) ref *6*, (– – –) ref *5*, (▲) ref *7*.

relevant literature values (*5–7*) are given in Table I and Figure 2. Over the range 300–600 °C in both argon and oxygen these data can be satisfactorily represented by the equation

$$\gamma(\text{dyn/cm}) = 133.12 - (6.25 \times 10^{-2})T(°C) \qquad (6)$$

with an uncertainty of ±0.5%. Each data point is the average of 10 measurements of the surface tension with a standard deviation of 0.2% for each set of measurements. The data shown in Figure 2 represent two independent experiments and provide an indication of the precision of the measurements.

The excellent agreement between our data and those of Krivovyazov et al. (*6*) and Ejima (*7*) (Table I and Figure 2) suggests that the data of ref *5* are incorrect. The agreement between these two sets of data is particularly reassuring since the data of ref *6* and *7* were obtained by a different method, maximum bubble pressure vs. plate detachment. A more complete discussion of this difference is given in ref *1*. As an additional check on the accuracy of our surface tension measurements, the surface tension of KNO_3 was determined. The results were well within the previously determined experimental uncertainty of 0.5% (Table II).

The effect of additions of KNO_2 on the surface tension of the binary $NaNO_3$–KNO_3 melt at 400 and 550 °C is shown in Table III. Within experimental uncertainty, the surface tension is unchanged even up to concentrations as large as 40 mol % KNO_2. This result is not unreasonable since the nitrates have a lower surface tension than the corresponding nitrites and thus

Table II. Surface Tension of KNO_3

T, °C	γ(exptl), mN/m	γ(lit.),[a] mN/m	T, °C	γ(exptl), mN/m	γ(lit.),[a] mN/m
374	108.5	108.3	450	103.3	102.8
401	106.2	106.4	474	100.6	101.1
425	104.3	104.6	500	99.8	99.3

[a] Reference *8*.

Table III. Effect of KNO_2 on the Surface Tension of $NaNO_3$-KNO_3

T, °C	KNO_2, mol %	γ, mN/m	T, °C	KNO_2, mol %	γ, mN/m
400	0	108.1	550	0	98.8
	10	109.0		10	99.2
	20	108.3		20	98.7
	40	108.7		40	98.1

Table IV. Density of Equimolar $NaNO_3$-KNO_3

T, °C	ρ(exptl), g/cm³	ρ(lit.),[a] g/cm³	T, °C	ρ(exptl), g/cm³
298	1.895	1.900[b]	498	1.774
347	1.873	1.872	555	1.735
400	1.836	1.835	595	1.709
442	1.810	1.805		

[a] Reference *5*. [b] Extrapolated.

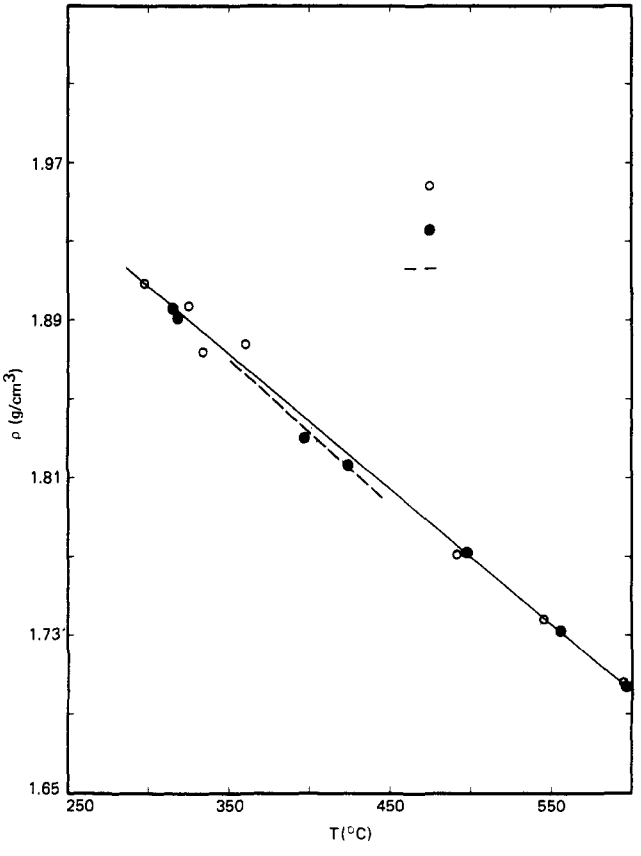

Figure 3. Density of $NaNO_3$–KNO_3 vs. temperature: (O) O_2, (●) Ar, (– – –) ref *5*.

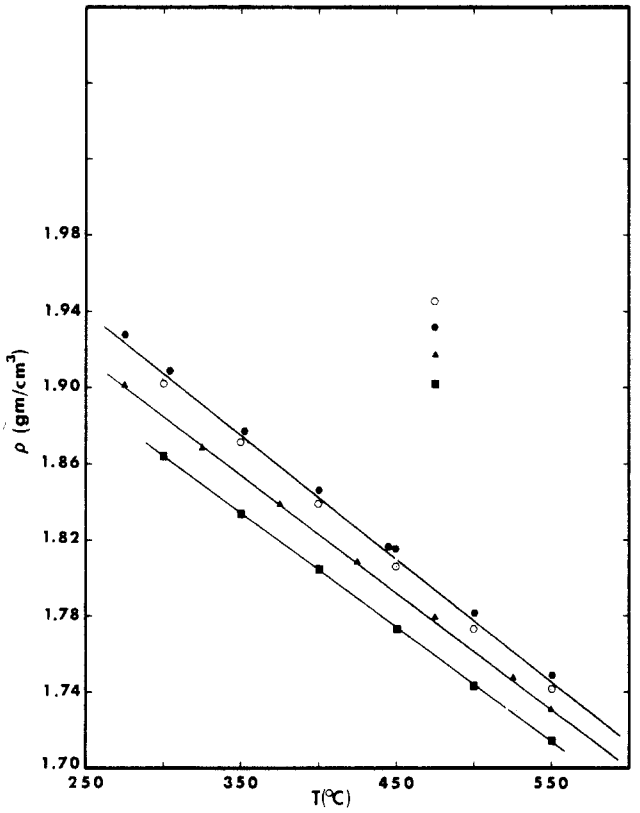

Figure 4. Density of $NaNO_3$–KNO_3–KNO_2 mixture vs. temperature: (O) 0, (●) 10, (▲) 20, and (■) 40 mol % KNO_2.

would tend to concentrate at the surface (*9*).

Density. The density of the equimolar $NaNO_3$–KNO_3 mixture in argon or oxygen is presented in Table IV and Figure 3 and compared with existing literature data (*5*). The experimental data can be represented by the equation

$$\rho(g/cm^3) = 2.090 - (6.36 \times 10^{-4})T(°C) \quad (7)$$

with an uncertainty of ±0.5% from 300 to 600 °C. The agreement between our experimental data and the literature values is excellent, being well within the 0.5% experimental uncertainty.

In contrast to the surface tension and the viscosity, which will be discussed later, the density shows a slight dependence upon the nitrite concentration for nitrite concentrations greater than 10 mol %. This is illustrated in Figure 4 for 10, 20, and 40 mol % nitrite/nitrate mixtures.

Viscosity. The viscosity of the equimolar $NaNO_3$–KNO_3 mixture between 300 and 600 °C, in argon and oxygen, is shown in Figure 5. For comparison, values of the viscosity from ref *5* are included. To facilitate comparison the solid line in Figure 5 is drawn through the literature data. It can be seen that agreement between the two sets of values is quite good. The viscosity may be calculated from the equation

$$\eta(\text{mPa s}) = 22.714 - 0.120T + (2.281 \times 10^{-4})T^2 - (1.474 \times 10^{-7})T^3 \quad (8)$$

for T in °C, with an uncertainty of 1.0%. Each value of the viscosity is the average of 10 separate measurements. The standard deviation of the logarithmic decrement is 0.2% with a standard deviation of 0.5% in the corresponding value of the viscosity. A total of 36 separate data points from five independent experiments were used to derive eq 8. The experimental viscosity data are given in Table V. Within the limits of experimental uncertainty, the presence of up to 40 mol % nitrite has no effect on the viscosity of the binary $NaNO_3$–KNO_3 mixture (Table VI).

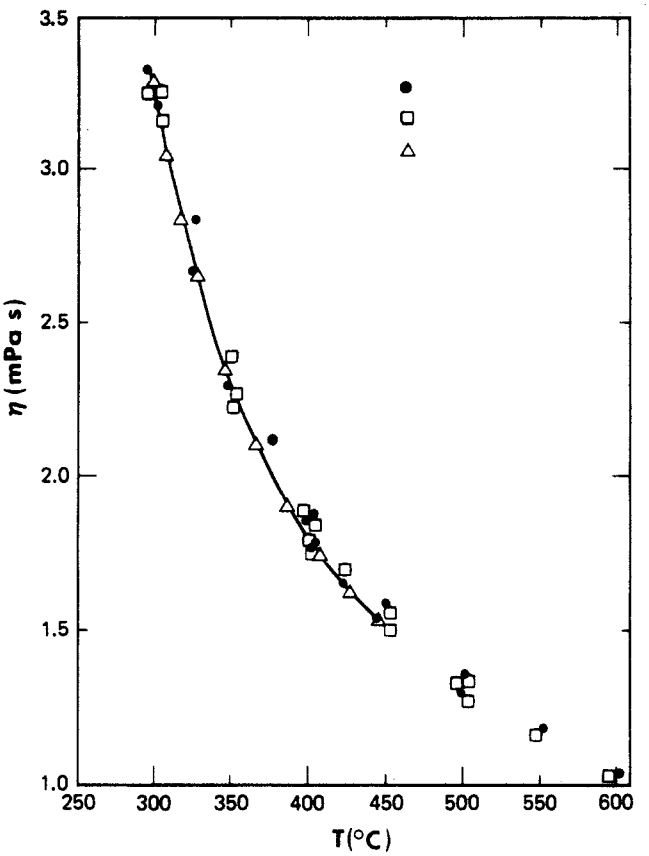

Figure 5. Viscosity of $NaNO_3$–KNO_3 vs. temperature: (●) O_2, (□) Ar, (△) ref *5*.

Table V. Experimental Viscosity Data

T, °C	η, mPa s	T, °C	η, mPa s
600	1.025	302	3.162
575	1.100	424	1.688
298	3.238	349	2.307
350	2.284	294	3.322
400	1.766	401	1.801
502	1.286	300	3.203
599	1.029	399	1.767
555	1.116	325	2.659
549	1.175	400	1.792
454	1.511	601	1.032
323	2.259	501	1.299
300	3.252	500	1.299
400	1.777	450	1.517
497	1.334	401	1.771
501	1.304	375	2.115
451	1.565	275	4.170
399	1.808		
402	1.771		
352	2.231		

Table VI. Effect of KNO_2 on the Viscosity of $NaNO_3$-KNO_3

T, °C	KNO_2, mol %	η,[a] mPa s	T, °C	KNO_2, mol %	η,[a] mPa s
400	0	1.78	550	0	1.19
	10	1.79		10	1.18
	20	1.80		20	1.20
	40	1.81		40	1.19

[a] 1 mPa s = 1 cP.

Summary

We have determined the viscosity, the surface tension, and the density for the equimolar mixture $NaNO_3$–KNO_3 in both argon and oxygen. Both the surface tension and the viscosity of this salt mixture are unaffected by concentrations of nitrite,

formed by thermal decomposition of nitrate, up to 40 mol %.

Acknowledgment

I acknowledge the assistance of K. E. Gels in fabricating the experimental apparatus and D. C. Macmillan in designing and programming the microprocessor.

Literature Cited

(1) Nissen, D. A. "A Single Apparatus for the Precise Measurement of the Physical Properties of Liquids at Elevated Temperature and Pressure," SAND80-8034; Sandia Laboratories: Livermore, CA, Oct 1980.
(2) Solomons, C.; White, M. S. *Trans. Faraday Soc.* **1969**, *65*, 309.
(3) Nissen, D. A.; Meeker, D. E. "Analytical Method for Nitrate Melts", in press.
(4) Nissen, D. A. "The Chemistry of the Binary $NaNO_3$–KNO_3 System", SAND81-8007; Sandia Laboratories: Livermore, CA, June 1981.
(5) Janz, G. J.; Krebs, U.; Siegenthaler, H. E.; Tomkins, R. P. T. *J. Phys. Chem. Ref. Data* **1972**, *1*, 587.
(6) Krivovyazov, E. L.; Sokolova, I. D.; Voskresenkaya, H. K. *J. Appl. Chem. USSR (Engl. Transl.)* **1963**, *36*, 2458.
(7) Ejima, T.; Nakamura, E. *J. Jpn. Inst. Metl. Sendai* **1975**, *39*, 680.
(8) Janz, G. J. *J. Phys. Chem. Ref. Data* **1980**, *9*, 909.
(9) Bloom, H.; Davis, F. G.; James, D. W. *Trans. Faraday Soc.* **1960**, *56*, 1179.

Received for review October 9, 1981. Accepted March 15, 1982.

Flammability Properties of Acrylonitrile and Acetonitrile

Silvio De Michell* and Vittorio Tartari

Montedipe S.p.A., Research Center, 20020 Bollate (Milan), Italy

Flammability limits were determined for ternary mixtures of acrylonitrile–air–nitrogen, acetonitrile–air–nitrogen, and acetonitrile/water (azeotropic ratio)–air–nitrogen. For the acrylonitrile–air system, slightly wider limits than those reported before were found. Maximum safe values for oxygen contents are also reported.

Introduction

In order to define the potential "plant hazard", flammability data are necessary for the pure compounds and the mixtures involved in every chemical process. Lower and upper flammability limits (LFL and UFL, respectively) in air, flammability limit curves vs. added inert concentration, and minimum oxygen content are usually required at the pressure and temperature levels occurring in the plant.

If literature data are missing, or incomplete, or obtained by means of an improper experimental apparatus, new experimentation is needed, since methods have not yet been developed for calculating flammability limits theoretically.

Although acrylonitrile (AN) and acetonitrile (AcN) are very common chemicals, only the upper and lower limits for the former were measured (*1*). These data are inadequate to solve all safety problems in propylene ammoxidation plants, where both chemicals are produced and stored.

In this work we have defined the flammability fields for the pure compounds and for the AcN/water azeotrope in air–nitrogen mixtures.

Experimental Section

The apparatus used for the flammability limits determination is shown in Figure 1. Gaseous streams were taken from cylinders or from the laboratory supply and metered through flowmeters. The liquid phase was fed to a vaporizer by means of a reciprocating pump and dosed by a buret. Punched plates were inserted along the feeding lines to improve the turbulence.

The global stream was carefully mixed into a mixer. Feeding lines were kept to such a temperature level that vapor condensation could be avoided.

The test vessel consists of a stainless-steel tube 5-cm i.d. and 150 cm long so thick that it could withstand the mechanical and thermic solicitations resulting from flammability tests. The size of our vessel is analogous to those reported elsewhere (*1*). The influence exerted on flammability limits by inner diameters smaller than 5 cm is well-known (*1*).

A rupture disk is mounted at the bottom of the vessel to allow the rapid discharge of possible overpressures. During the discharge time the vessel can be bypassed without influencing the gaseous stream composition: this procedure allows one to carry out many tests with the same mixture.

If necessary the vessel can be heated electrically. The state of the temperature inside the vessel was monitored by the thermocouples shown in Figure 1.

The pressure was kept to a constant level by means of a volumetric valve situated at the top of the vessel.

Mixtures were ignited by an inductive spark located in the middle of the vessel. The igniter consists of two stainless-steel wire electrodes held by a tubular Teflon piece and spaced 2 mm apart. The wires are connected to a 50-cycles transformer, operating at 220-V input, 12 000-V output. An energy of 20 J was released during the discharge time, which was held constant at ~50 ms. The mixture to be tested could be sampled at the inlet, at the middle, and at the outlet of the vessel, in order to control the homogeneity of the composition all along the vessel. The volumetric composition of the mixture was determined by using an on-line gas chromatograph.

The propagation of the flame was detected by two 0.1-mm gauge Pt–Rh 6%/Pt–Rh 30% thermocouples extending into the vessel to a point about 10 mm from the vertical axis of the vessel. These thermocouples have a very low time constant (0.07 s).

During these tests we considered only upward flame propagation. It is known that the limits measured under these conditions are wider than those determined under any other condition.

The rapid output generated by the thermocouples was stored on a variable-frequency transient recorder and afterward was replotted on a two-channel chart recorder. Start, duration, and power of the electrical discharge were monitored on the same recorder.

Owing to the low threshold limiting value (TLV) fixed for these compounds (TLV proposed for AN = 1–2 ppm), the vent line discharged into a torch and gases were burned carefully.

The equipment and the feeding pump were installed into a heavily constructed pressure box and were operated from outside, so that the operator was fully protected from any

0021-9568/82/1727-0273$01.25/0